QUANTITATIVE CHARACTERIZATION OF A BIOLOGICAL MEMBRANE BY MEANS OF ITS SPATIAL AUTOCOVARIANCE

G. RASIGNI,* J. PALMARI,* M. RASIGNI,* F. VARNIER,* J. P. PALMARI,* F. MARTY,‡ AND
A. LLEBARIA§
*Départment de Physique des Interactions Photons-Matière, Faculté des Sciences St Jérôme, 13397
Marseille Cedex 13, France; ‡Institut de Cytologie et de Biologie Cellulaire, Faculté des Sciences de
Luminy, 13288 Marseille Cedex 9, France; and §Laboratoire d' Astronomie Spatiale, 13012 Marseille,
France

ABSTRACT   Profiles for the exoplasmic face (EF) of the freeze-fractured plasma membrane from the root storage tissue of red beets are reconstructed by microdensitometry of micrographs of surface–shadowed-platinum carbon replicas. Autocovariance functions (ACFs) are computed from those profiles. The initial portions of the ACFs have a Gaussian form whose parameters (root mean square surface roughness and autocovariance length) are estimated. The parameter estimates are used to show that the pits on the EF faces are in good complementarity with the intramembrane particles seen on the complementary protoplasmic fracture faces.

INTRODUCTION

Frozen biological membranes maintain their in vivo organization. Their freeze fracture provides much valuable information about their internal organization because in the fracturing process they are split into two halves, thus exposing extended face views of their hydrophobic interiors (1). The most distinctive structural features seen on fracture-face replicas are prominent intramembrane particles and a relatively smooth background matrix. Although much attention has been focused on the intramembrane particles, the relief of the matrix has not been ignored (2, 3). Under optimal conditions, it shows numerous pits (4) whose origins are not fully understood. On some fracture faces these pits have either been shown to match particles on the complementary fracture face or have been ascribed to some contaminant. Under our experimental conditions ($-110°C$, 10^{-6} torr), the pits observed on the fracture faces cannot be attributed either to surface etching and recondensation or to cleavage and replicating procedures, for the following reasons: (a) the pits are located on the exoplasmic fracture faces (EF) but are absent from the protoplasmic fracture faces (PF). (b) The pits appear to be different on vacuole and plasma membrane EF faces. (c) The pits on the EF faces appear to be in good complementarity with the intramembrane particles seen on the complementary PF faces. Until now, a good complementarity has been demonstrated only by matching areas of high-quality double replicas. (d) The fracture through the frozen membrane exposes the hydrophobic portion of nonvolatile constituents; therefore, the sublimation rate should be minimal and the exposed faces practically unetchable at low temperature and high vacuum.

Methods for characterizing and analyzing membrane structures have been the subject of considerable interest since the invention of freeze-etch techniques (5). Recent progress has awaited the development of new methods particularly suitable for the quantitative characterization of the lipid matrix of membranes (6–8).

Recently, Rasigni et al. (9–18) developed a method for studying the surface roughness of various surfaces. In this method, electron-micrographs of shadowed-surface replicas are analyzed by microdensitometry. The surface relief is reconstructed line by line, making the computation of the autocovariance function (ACF), which statistically describes the surface, possible. The rationale of the present study lies in the assumption that the fracture face of a frozen biological membrane may be considered as any
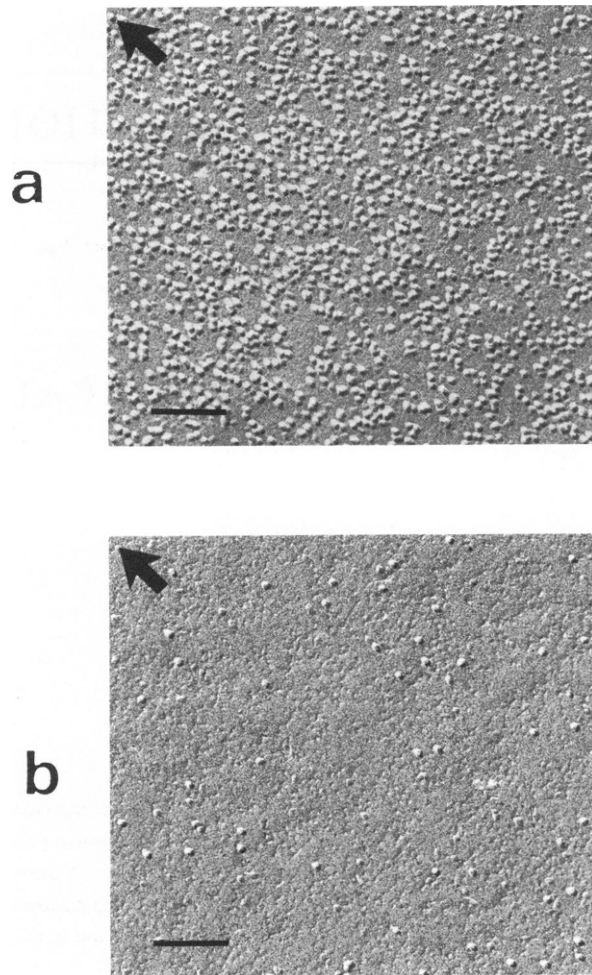
FIGURE 1 Photomicrographs of shadowed-platinum carbon replicas of the freeze-fracture faces from plasma membrane of red beet cells. (a) PF face. (b) EF face. The line represents 0.1 μm.

other rough surface, and, therefore it can be characterized by its ACF. From its ACF, one can deduce the root mean square (rms) variation in the height of the surface about its mean (rms δ) and a measure of the distance over which the structure is correlated along the mean surface (autocovariance length σ). Here we show that the initial portion of ACFs for the background matrix of the plasma membrane from red beets have a Gaussian form and the values of δ(5.6–6.5 Å) and σ(32–44 Å) are estimated. Moreover, the ACFs for the PF faces and EF faces show that the pits on the EF faces and the intramembrane particles on the PF faces exhibit a close fit in their statistical distribution.

MATERIALS AND METHODS

The present study is focused on the quantitative characterization of the background matrix of the plasma membrane from root storage tissue of red beets. The exoplasmic fracture (EF) faces of this membrane contain a sparse population of intramembrane particles. Therefore it is possible to scan extensive areas free from particles and to obtain data only related to the background matrix.

The samples were prepared in the following way. Small blocks (~1 mm³) from the root storage tissue of red beets (*Beta vulgaris* L. var. *esculenta* Gürke) were chemically stabilized for 15 min at room temperature with 3% (vol/vol) glutaraldehyde 1.5% (wt/vol) paraformaldehyde in 50 mM cacodylate buffer, pH 7.3. Fixation was routinely used because freeze-fractured specimens from bulky tissues appeared better preserved in aldehyde-fixed tissues than in unfixed ones. The samples were washed three times in 100 mM cacodylate buffer pH 7.3, containing 0.2 M sucrose, for 15 min each, then infiltrated with 25% (vol/vol) glycerol in cacodylate buffer, for 1 h at room temperature. Samples were frozen at liquid nitrogen temperature in the infiltration medium and freeze-fractured at −110°C. Replicas were prepared according to standard procedures on a Balzers freeze-etching apparatus (BAF 300; Balzers Union, Liechtenstein) equipped with electron-beam guns (EK 552, Balzers Union) for Pt/C (95:5) and carbon depositions. The three plasma membrane EF faces and the PF face studied in this paper were from different tissue samples prepared under identical fracturing conditions.

The two-dimensional analysis of electron micrographs is carried out with a processing data-system microdensitometer (1010 A; Perkin-Elmer Corp., Instrument Division, Norwalk, CT) that measures the micrograph density d at regular intervals in both the x (shadow direction) and the y
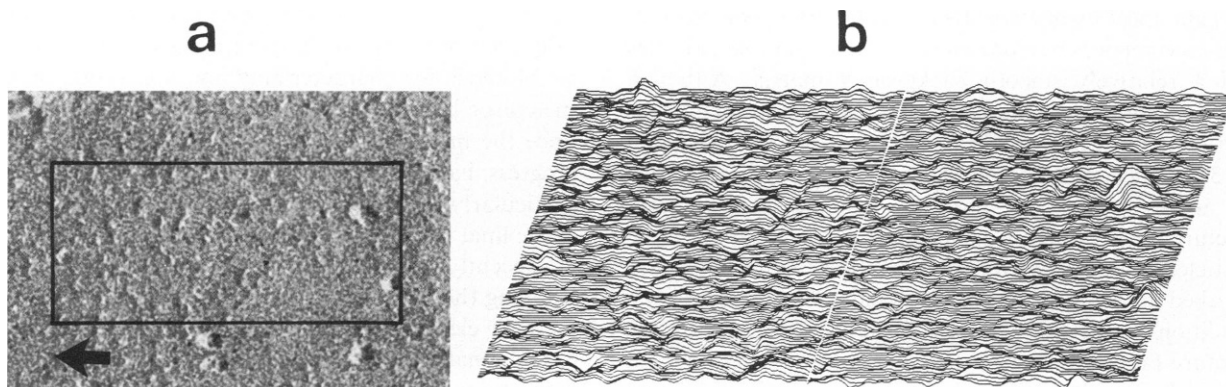

FIGURE 2 (a) Photomicrograph for one of the three EF faces studied here. Framed area side 0.2 μm × 0.1 μm. (b) Perspective view of the surface a obtained by microdensitometer analysis using a computer plotting program. The plot consists of 250 lines, 500 points/line. For convenience only one line out of two is shown. The perspective angle is 18°. The area represented in b is the framed one shown in a.

TABLE I
CHARACTERISTICS OF THE MICRODENSITOMETER RECORDING PROCESS

Surfaces	Micrograph magnification	Scanning spot area		x and y increments		Number of points per line	Number of lines	Window bidimensional filtering	Window unidimensional filtering
		a^*	$b\ddagger$	a^*	$b\ddagger$				
EF faces*		μm^2	$\mathring{A}^2$	μm	$\mathring{A}$				
(a)	×25,000	10 × 10	4 × 4	10	4	1,800	250	4 × 4	100
(b)	×25,000	10 × 10	4 × 4	10	4	1,600	250	4 × 4	100
(c)	×25,000	10 × 10	4 × 4	10	4	1,500	200	4 × 4	80
PF face	×25,000	30 × 30	12 × 12	30	12	1,540	250	4 × 4	31

*a relates to microdensitometer optics. $\ddagger b$ represents corresponding values on the real surface, taking into account micrograph magnification.

direction, producing a grid of L scanning lines with N pixels per line. We showed previously (9) that the slopes p of the surface elements are proportional to the micrograph density d. Thus, the surface profile for a line may be obtained by integrating the density data $d(x)$. Different filtering algorithms have to be used in order to eliminate random noise (9). Recently the method has been improved (17) and we are now able to detect very fine details on the surface. Fig. 9 in reference 9 and Fig. 2 in reference 17 summarize the different steps leading to the determination of the surface profiles.

RESULTS AND DISCUSSION

Fig. 1 illustrates the typical freeze-fracture faces of the plasma membrane of beet root cells. The PF face contains a dense population of particles on a relatively smooth background (Fig. 1 a). The complementary EF face (Fig. 1 b) looks strikingly different, with a sparse population of particles on a background matrix made rough by numerous small depressions or pits.

Fig. 2 a shows the photomicrographs of the EF face from one of the three samples we have studied in this paper. The principal characteristics connected with the micrograph analysis are reported in Table I. The characteristics of windows related to the median filtering (9) are also reported in the table. It is possible to visualize the reconstruction of surface profile obtained by microdensitometer analysis in plotting successive tracings of lines, each displaced to establish a perspective view of the surface. Fig. 2 b shows such a reconstruction for a part of the surface represented in Fig. 2 a.

From the restored profile one can estimate the moments that summarize statistical information on the various characteristic lengths describing the surface. We assume
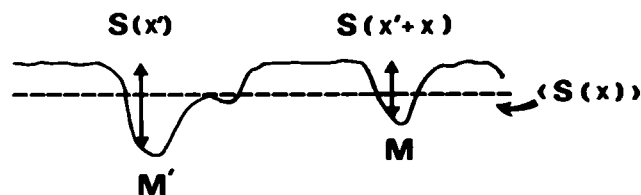
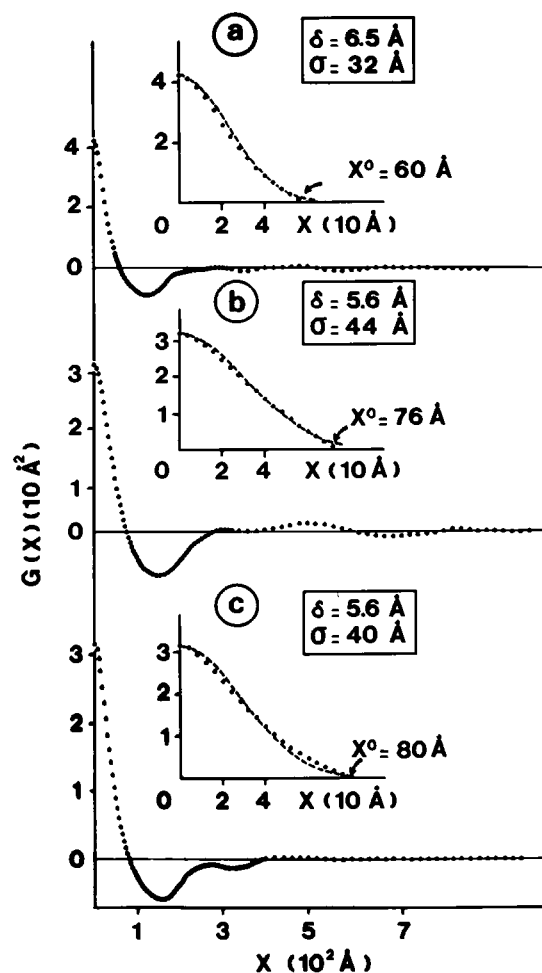FIGURE 3   Profile of a rough surface.

FIGURE 4   ACF for the three surfaces studied here. Results are given as averages over 60 lines. ACFs were computed by using the FFT algorithm. Number of pixels per line: (a) 1,792, (b) 1,536, (c) 1,280. Number of points correlated: 256. Initial portions of $G(x)$ are reported on an expanded x scale, and the dashed curves are Gaussian functions $G(x) = \delta^2 \exp(-x^2/\sigma^2)$, with values of δ and σ given in the figure.

that the surface of the background matrix is isotropic (see Fig. 1), so we limit our discussion to one dimension. Let $S(x)$ be the profile in a straight line (Fig. 3). In the case of a statistically rough surface the function $S(x)$ is often described by the first two moments

$$\langle S(x) \rangle, \tag{1}$$

$$\langle S(x) \, S(x') \rangle, \tag{2}$$

where the angular brackets denote an average over the ensemble of realizations of the function $S(x)$. If we consider deviations from the height of the surface with respect to a plane defined (Fig. 3) by the average height $\langle S(x) \rangle$, namely

$$H(x) = S(x) - \langle S(x) \rangle, \tag{3}$$

we have for the first-order moment

$$\langle H(x) \rangle = 0, \tag{4}$$

and the second-order moment

$$\langle H(x) \, H(x') \rangle, \tag{5}$$

is called the ACF. Assuming that the membrane is isotropic, the ACF depends on x and x' only through their difference, and the autocovariance becomes

$$G(x) = \langle H(x') \, H(x' + x) \rangle, \tag{6}$$

which we estimate from the data as

$$G(x) = \frac{1}{N - x} \sum_{x'=1}^{N-x} H(x') \, H(x' + x), \tag{7}$$

where x' indexes the pixels along a line.

The convolution given by Eq. 7 was computed by using the Cooley-Tukey fast Fourier transform (FFT) algorithm (14, 15). We noted that the behavior of the ACF depends on the line considered so that good estimates are obtained only if results are given as averages over a large number of widely spaced lines ($\sim$60 lines in the present study). We also found that $G(x)$ is insensitive to N if N is at least 1,024. Fig. 4 shows the ACFs for the three fracture areas we have studied. The initial portions of $G(x)$ reported on an expanded scale are fairly close to Gaussian, namely

$$G(x) = \delta^2 \exp(-x^2/\sigma^2), \tag{8}$$

where δ is the rms defined as $G(o) = \delta^2$ and σ is defined to be the autocorrelation length. The expression (Eq. 8) is only valid (see Fig. 4) when x does not exceed (a) 56 Å, (b) 68 Å, and (c) 76 Å. The values of δ and σ are reported in Fig. 4. Another useful parameter to specify besides δ and σ is x°, the value of x for which the autocovariance function $G(x) = 0$. Values of x° are also reported on (Fig. 4). Pits that are seen in Fig. 2 a that have lateral dimensions of $\sim$30–60 Å are characterized in the $G(x)$ curve by a σ of 40 Å. The $G(x)$ curves oscillate with a periodicity $\simeq$220–260 Å that approximately corresponds to the mean distance between the pits. Because of the randomness of the pits, the ACFs are almost completely damped out for $x \simeq 700$ Å, showing progressively weaker dependence between the observations as the distance between them increases. We conclude that the values $\delta \simeq 6$ Å, $\sigma \simeq 40$ Å, and $x^\circ \simeq 70$ Å are characteristics of the background matrix of the EF faces of the plasma membrane from red-beet storage tissue. These values should be useful, not only as intrinsic structural markers for this membrane, but also as quantitative parameters of the components responsible for the relief. To date, the origin of the pits located on the
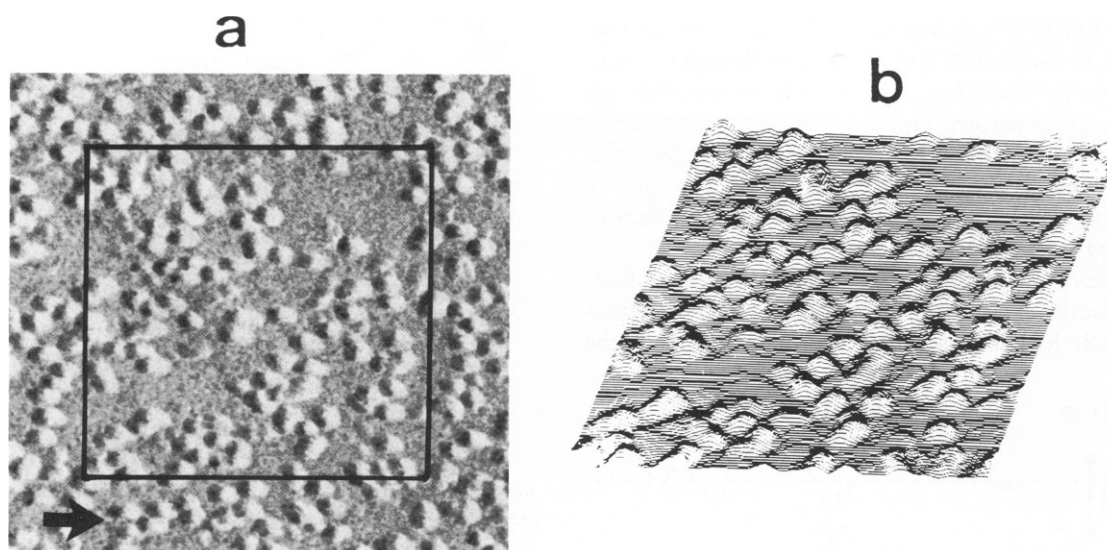

FIGURE 5 (a) Photomicrograph for the PF face studied here. Framed area side 0.18 μm. (b) Perspective view of the surface a obtained by microdensitometer analysis using a computer plotting program. The plot consists of 150 lines, 150 points/line. The perspective angle is 18°. The area represented in b is the framed one shown in a.
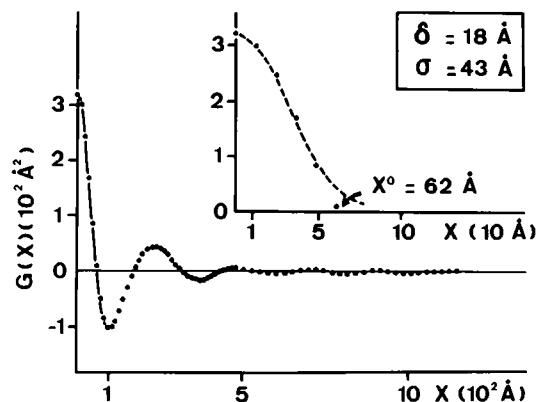
FIGURE 6   ACF for a PF face. Result is given as average over 63 lines. ACF was computed by using FFT algorithm. Number of pixels per line: 1,536. Number of points correlated: 256. The initial portion of $G(x)$ is reported on an expanded x scale and the dashed curve is the Gaussian function $G(x) = \delta^2 \exp(-x^2/\sigma^2)$ with values of δ and σ given in the figure.

background matrix is not understood. These pits might result from (a) clusters of distinct lipids with short fatty acid chains in the membrane core; (b) lipid or protein regions that are traversed by covalently bonded components and thus submitted to plastic distorsion during the fracture process; (c) the impression left in the lipid matrix by the particles seen on the complementary fracture face. This is the usual hypothesis when the roughness of the background is being considered. We have undertaken the study of the PF face to check this hypothesis on statistical grounds.

Fig. 5 a shows the photomicrograph for a PF face (originating from a different sample from that used for Fig. 4) and Fig. 5 b is the reconstruction obtained by the process just described. For convenience, only a part of the surface is represented. The principal characteristics connected with the micrograph analysis are reported in Table I. From the restored profile we have computed the ACF shown in Fig. 6. The initial portion of $G(x)$ reported on an expanded scale is again fairly close to a Gaussian, from which we estimate $\delta = 18$ Å and $\sigma = 43$ Å. The value of σ is close to the one deduced from the ACFs related to the EF faces. Moreover $G(x)$ oscillates with a periodicity $\simeq 230$–240 Å, which is similar to the period observed in the ACF of the EF face. Since these statistical properties of pits and intramembrane particles are similar, we may conclude that there is a complementarity of the fracture faces. However, the δ values for the complementary faces are different. The discrepancy could be related to the plastic deformation of membrane components, although tenuous shadowing and contamination impairments cannot be totally ruled out (19).

CONCLUSION

We have shown that it is possible to reconstruct the surface profile of a biological membrane and to deduce the ACF

that statistically characterizes the surface. The method we have used, namely, a microdensitometer analysis of electron micrographs of surface replica, is not new, but has not to our knowledge been applied to the study of freeze-fracture membranes. The difference between our method and those in references 20–24 is that we have implemented filtering algorithms that are necessary to eliminate random noise. We have shown in reference 9 that the profile obtained from direct integration of the microdensitometer data without filtering is different from the profile obtained using median filtering, and so are the ACFs. The statistical properties of a membrane surface can be approached in different ways. For the membranes in Figs. 1 a and 5, point-counting methods might be just as appropriate as the method described here. However, for the membranes shown in Figs. 1 b and 2, measures of texture such as those that we have described may be the only sensible way to characterize the membrane.

REFERENCES

1. Branton, D. 1966. Fractures faces of frozen membranes. Proc. Natl. Acad. Sci. USA. 55:1048–1056.
2. Verkleij, A. J., and P. H. Th. Ververgaert. 1978. Freeze fracture morphology of biological membranes. Biochim. Biophys. Acta. 515:303–327.
3. Benedetti, E. L., and P. Favard, editors. 1973. Freeze Etching Techniques and Applications. Societé Française de Microscopie Electronique. Paris.
4. Marty, F. 1982. Isolation and freeze-fracture characterization of vacuole membrane fragments. In Plasmalemma and Tonoplast: Their Functions in the Plant Cell. D. Marmé, E. Marre, and R. Hertel, editors. Elsevier Biomedical Press, Amsterdam. 179–188.
5. Staehelin, L. A. 1973. Analysis and critical evaluation of the information contained in freeze-etch micrographs. In Freeze Etching Techniques and Applications. E. L. Benedetti, and P. Favard, editors. Societé Française de Microscopie Electronique. Paris. 113–134.
6. Edelman, J. 1982. Theory of protein influence on membrane thickness. Biophys. J. 37:143–144.
7. Crilly, J. F., and J. C. Earnshaw. 1983. Photon correlation spectroscopy of bilayer lipid membranes. Biophys. J. 41:197–210.
8. Pearson, T., and S. I. Chan. 1982. Effects of lipid-mediated interactions on protein pair distribution functions. Biophys. J. 37:141–142.
9. Rasigni, M., G. Rasigni, J. P. Palmari, and A. Llebaria. 1981. Study of surface roughness using a microdensitometer analysis of electron micrographs of surface replicas. I. Surface profiles. J. Opt. Soc. Am. 71:1124–1133.
10. Rasigni, M., G. Rasigni, J. P. Palmari, and A. Llebaria. 1981. Study of surface roughness using a microdensitometer analysis of electron micrographs of surface replicas. II. Autocovariance functions. J. Opt. Soc. Am. 71:1230–1237.
11. Rasigni, M., F. Varnier, G. Rasigni, J. P. Palmari, and A. Llebaria. 1981. Validity of surface roughness study using microdensitometer analysis of electron micrographs of surface replicas. J. Opt. Soc. Am. 71:1549–1550.
12. Rasigni, G., F. Varnier, M. Rasigni, J. P. Palmari, and A. Llebaria. 1982. Autocovariance function, root-mean-square roughness height and autocovariance length for rough deposits of copper, silver and gold. Phys. Rev. B. 25:2315–2323.

13. Varnier, F., M. Rasigni, G. Rasigni, J. P. Palmari, and A. Llebaria. 1982. Height and slope distributions for surfaces of rough metallic deposits. *Appl. Opt.* 21:3681–3684.
14. Rasigni, G., F. Varnier, M. Rasigni, J. P. Palmari, and A. Llebaria. 1983. Autocovariance functions for polished optical surfaces *J. Opt. Soc. Am.* 73:222–233.
15. Rasigni, G., F. Varnier, M. Rasigni, J. P. Palmari, and A. Llebaria. 1983. Roughness spectrum and surface plasmons for surfaces of silver, copper, gold, and magnesium deposits. *Phys. Rev. B.* 27:819–830.
16. Rasigni, G., F. Varnier, M. Rasigni, J. P. Palmari, and A. Llebaria. 1983. Spectral-density function of the surface roughness for polished optical surfaces. *J. Opt. Soc. Am.* 73:1235–1239.
17. Varnier, F., G. Rasigni, M. Rasigni, J. P. Palmari, and A. Llebaria. 1984. Improvement in the reconstruction of surface profile deduced from microdensitometer analysis of electron micrographs of shadowed surface replicas. *J. Opt. Soc. Am. A* . 1:135–137.
18. Rasigni, G., F. Varnier, M. Rasigni, and A. Llebaria. 1984. Higher-order moments for profiles of statistically rough, real surfaces. *Phys. Rev. B.* 29:5931–5933.
19. Branton, D. 1973. The fracture process of freeze-etching. *In* Freeze Etching Techniques and Applications. E. L. Benedetti, and P. Favard, editors. Societé Française de Microscopie Electronique. Paris. 107–112.
20. Kistler, J., U. Aebi, and E. Kellenberger. 1977. Freeze-drying and shadowing a two-dimensional periodic specimen. *J. Ultrastruct. Res.* 59:76–86.
21. Smith, P. R., and J. Kistler. 1977. Surface reliefs computed from micrographs of heavy metal-shadowed specimens. *J. Ultrastruct. Res.* 61:124–133.
22. Krbecek, R., C. Gebhart, H. Gruler, and E. Sackmann. 1979. Three dimensional microscopic surface profiles of membranes reconstructed from freeze etching electron micrographs. *Biochim. Biophys. Acta.* 554:1–22.
23. Smith, P. R., and I. E. Ivanov. 1980. Surface reliefs computed from micrographs of isolated heavy metal shadowed particles. *J. Ultrastruct. Res.* 71:25–36.
24. Chalcroft, J. P. 1980. Three dimensional information from microdensitometer analysis of preshadowed replicas. *Mikroskopie (Wien).* 37(Suppl.):198–203.